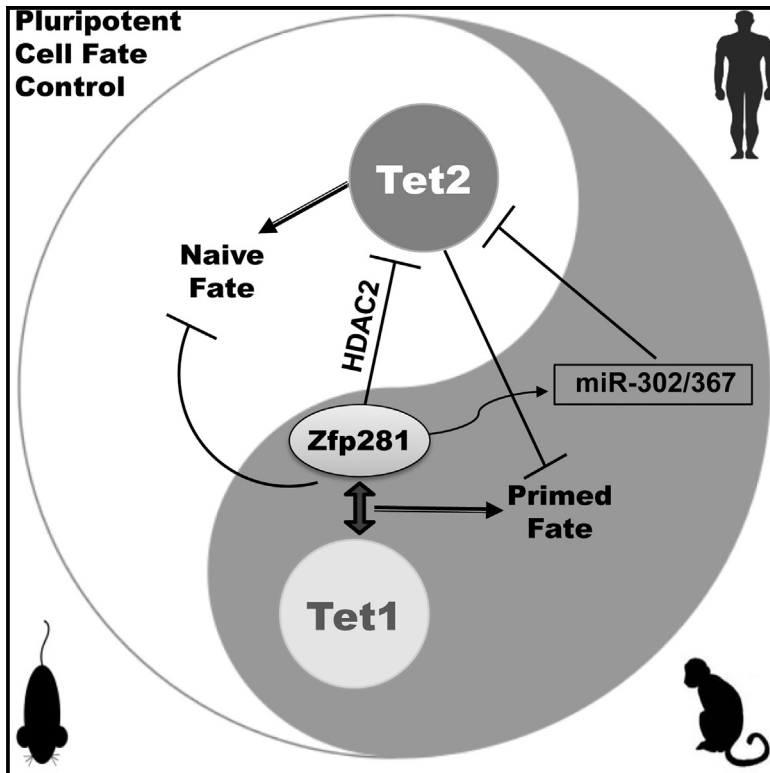Article

Zfp281 Coordinates Opposing Functions of Tet1 and Tet2 in Pluripotent States

Graphical Abstract

Authors

Miguel Fidalgo, Xin Huang,
Diana Guallar, ..., Wen-Shu Wu,
Carlos Clavel, Jianlong Wang

Correspondence

jianlong.wang@mssm.edu

In Brief

Wang and colleagues define an evolutionarily conserved pluripotent cell fate (PCF) gene signature that functionally distinguishes naive from primed cells. An RNAi screen for PCF gene regulators led to the discovery of opposing functions of Tet1 and Tet2 mediated by Zfp281 in transcriptional and post-transcriptional control of pluripotent states.

Highlights

- Identification of gene expression signatures for alternative pluripotent states

- Requirement of Zfp281 for the establishment and maintenance of primed pluripotency

- Opposite functions of Tet1 and Tet2 for primed and naive pluripotency

- Transcriptional and post-transcriptional repression of *Tet2* for primed pluripotency

Accession Numbers

GSE81045

CrossMark

CellPress

Zfp281 Coordinates Opposing Functions of Tet1 and Tet2 in Pluripotent States

Miguel Fidalgo,[1,2,3] Xin Huang,[1,2] Diana Guallar,[1,2] Carlos Sanchez-Priego,[1,2] Victor Julian Valdes,[1,2] Arven Saunders,[1,2,4] Junjun Ding,[1,2] Wen-Shu Wu,[5] Carlos Clavel,[6] and Jianlong Wang[1,2,4,*]

[1]The Black Family Stem Cell Institute, Icahn School of Medicine at Mount Sinai, New York, NY 10029, USA
[2]Department of Developmental and Regenerative Biology, Icahn School of Medicine at Mount Sinai, New York, NY 10029, USA
[3]Departamento de Fisioloxia, Centro de Investigacion en Medicina Molecular e Enfermidades Cronicas, Universidade de Santiago de Compostela, Santiago de Compostela 15782, Spain
[4]The Graduate School of Biomedical Sciences, Icahn School of Medicine at Mount Sinai, New York, NY 10029, USA
[5]Department of Medicine and Cancer Center, University of Illinois at Chicago, Chicago, IL 60612, USA
[6]Hair and Pigmentation Development, A*Star-Institute of Medical Biology, 138648 Singapore, Singapore
*Correspondence: jianlong.wang@mssm.edu
http://dx.doi.org/10.1016/j.stem.2016.05.025

SUMMARY

Pluripotency is increasingly recognized as a spectrum of cell states defined by their growth conditions. Although naive and primed pluripotency states have been characterized molecularly, our understanding of events regulating state acquisition is wanting. Here, we performed comparative RNA sequencing of mouse embryonic stem cells (ESCs) and defined a pluripotent cell fate (PCF) gene signature associated with acquisition of naive and primed pluripotency. We identify Zfp281 as a key transcriptional regulator for primed pluripotency that also functions as a barrier toward achieving naive pluripotency in both mouse and human ESCs. Mechanistically, Zfp281 interacts with Tet1, but not Tet2, and its direct transcriptional target, miR-302/367, to negatively regulate Tet2 expression to establish and maintain primed pluripotency. Conversely, ectopic Tet2 alone, but not Tet1, efficiently reprograms primed cells toward naive pluripotency. Our study reveals a molecular circuitry in which opposing functions of Tet1 and Tet2 control acquisition of alternative pluripotent states.

INTRODUCTION

Cell-fate decisions involve coordinated gene regulation at transcriptional and post-transcriptional levels, but the precise mechanisms underlying these complex processes are still poorly defined. Notably, manipulation of key signaling pathways is sufficient to force specific cell types to undergo global transcriptional changes in order to acquire new identities, including pluripotency (Chou et al., 2008). A great interest has thus emerged to understand how these alternative pluripotent identities are regulated (Weinberger et al., 2016; Wu and Izpisua Belmonte, 2015). In mouse embryonic stem cells (ESCs), standard culture conditions containing serum and leukemia inhibitory factor (LIF) (hereafter

"SL") support the self-renewal and maintenance of a heterogeneous or metastable pluripotent state (Marks et al., 2012). This in vitro cell identity can be reprogrammed into two inter-convertible and defined pluripotent states by activating distinct signaling pathways. Specifically, serum-free medium containing MEK and GSK3β kinase inhibitors and LIF (hereafter "2iL") supports naive pluripotency that mimics the naive inner cell mass (ICM) of the blastocyst (Nichols and Smith, 2009). Alternatively, a more committed primed pluripotent state resembling post-implantation epiblast cells can be induced in serum-free medium containing the cytokines fibroblast growth factor 2 (Fgf2) and Activin A (hereafter "FA") (Guo et al., 2009; Han et al., 2010).

The functional conservation of pluripotency hallmarks, i.e., unlimited self-renewal and differentiation into all somatic cell types, among these three pluripotent states (naive, metastable, and primed) suggests that common regulatory networks may participate in the pluripotent cell fate (PCF) determination. Considerable progress has been made in identifying transcriptional and epigenetic regulators required for maintenance of gene expression patterns associated with pluripotency identity, mainly under SL and 2iL conditions (Hackett and Surani, 2014). However, our knowledge regarding the molecular players responsible for re-wiring the epigenome for proper transcriptional and epigenetic control of naive and primed cell fate acquisition is still limited.

Manipulation of specific signaling cues to directly induce SL ESCs toward naive (2iL) or primed (FA) pluripotent states provides an opportunity to dissect the molecular mechanisms underlying PCF determination. Here, by using this experimental system, we identified the expression pattern of gene sets associated with naive and primed cell identities, referred to as PCF gene signature hereafter, which was found to be evolutionarily conserved in mammals. Using this PCF gene signature as the discovery tool, we performed an RNAi screen to search for transcriptional and epigenetic regulators that control the two pluripotent state transitions. We report here our findings of opposing functions of DNA dioxygenases Tet1 and Tet2 in regulating primed and naive pluripotency, respectively, and of Zfp281 as a key pluripotency factor that coordinates Tet1 and Tet2 functions, transcriptionally and post-transcriptionally, in activation of primed genes and repression of naive genes for primed pluripotency.

RESULTS

Identification of a PCF Gene Signature for Alternative Pluripotent States

To deconstruct the complex and dynamic processes involved in global gene expression changes for alternative pluripotent states, we reasoned that identification of distinct gene expression patterns in response to 2iL and FA signaling pathways could provide insight into the regulatory networks governing naive and primed PCF acquisition. We first monitored the kinetics of direct conversion of SL ESCs to naive and primed pluripotent states with a GFP reporter under the control of the *Oct4* distal enhancer (*Oct4*-ΔPE-GFP) (Figure S1A), which is active in the 2iL and SL states but is extinguished in the primed epiblast (Bao et al., 2009). Flow cytometry analysis showed stable expression of GFP in ESCs grown in SL throughout multiple passages (Figure S1A). However, these ESCs displayed markedly different reporter activity under 2iL or FA conditions over extended passages (Figures S1A and S1B). In particular, we found that 48-hr culture was sufficient to increase or decrease *Oct4*-ΔPE-GFP activity by 50% under 2iL and FA, respectively, representing an ideal time frame to examine changes in gene expression associated with alternative PCF acquisition. We then performed RNA sequencing (RNA-seq) to characterize transcriptome changes of ESCs grown in SL upon transfer to 2iL and FA conditions for 48 hr. To identify genes that are most closely associated with naive and primed states, we compared these transcriptomes to those of ESCs cultured for 16 days in 2iL and to EpiSCs in FA culture conditions. Differential expression analysis revealed a set of 2,036 genes with dynamic expression patterns comprising two major groups (Figure 1A; Supplemental Experimental Procedures): (1) group 1 genes are upregulated or actively expressed during metastable to naive transition, encompassing two classes (I and II), and (2) group 2 genes are actively expressed or upregulated during metastable to primed transition, encompassing two additional classes (III and IV) (Table S1). While classes I and IV are induced in response to 2iL and FA, respectively, classes II and III are silenced in response to FA and 2iL, respectively. Principal-component analysis (PCA) of transcriptomes of our cultured cells and those of established ESCs and epiblast stem cells (EpiSCs) under 2iL and FA conditions revealed a better separation of naive and primed pluripotent cells based on our PCF signature genes than global transcripts (Figure 1B). Gene ontology (GO) analysis of these four classes of genes revealed a significant presence of GO terms linked to developmental processes (Figure S1C). While naive state active gene classes (I and II) are enriched for GO terms associated with metabolic processes, primed state active gene classes (III and IV) are enriched for post-implantation developmental terms, such as morphogenesis and gastrulation (Figure S1C). These pluripotent state associated GO terms are consistent with previously reported findings in naive 2iL ESCs (Marks et al., 2012) and are compatible with the transition into a developmentally primed state.

We next tested whether this PCF gene signature was consistent across multiple genetic backgrounds. Unbiased hierarchical clustering of the 2,036 differentially expressed genes using our own, as well as published, RNA-seq datasets from mouse ESC lines of various genetic backgrounds cultured for several passages in 2iL as well as EpiSC lines cultured in FA (Factor et al.,

2014; Marks et al., 2012; Wu et al., 2015) revealed that naive cells clustered together in a group distinct from primed cells (Figure S1D). Notably, similar results were also obtained by analyzing available transcriptomes of in vivo mouse naive ICM and post-implantation primed epiblast (Brons et al., 2007) (Figure 1C, top). Cross-species comparison of the expression of human and monkey orthologs of 2,036 mouse genes (Chan et al., 2013; Chen et al., 2015; Wu et al., 2015) demonstrated that the identified PCF gene signature could also distinguish naive from primed primate cells (Figure 1C, middle and bottom).

Together, our studies reveal a novel and dynamic PCF gene expression signature associated with naive and primed pluripotency transitions that is evolutionarily conserved across different species and genetic backgrounds. This PCF gene signature provides a tool for interrogating molecular regulators that orchestrate pluripotent state transitions.

Zfp281 Contributes to PCF Signature Gene Regulation

To search for master regulators that control this newly defined PCF gene signature, we performed chromatin enrichment analysis using the Network2Canvas computational tool for a large number of transcription factors (TFs) and chromatin regulators in ESCs (see Supplemental Experimental Procedures). We observed the separation of enrichment patterns according to the pluripotent states. That is, naive classes I and II (group 1) and primed classes III and IV (group 2) are more similar within the group than across groups (Figure S2A). Notably, we observed that the core pluripotency factors Oct4, Sox2, and Nanog (OSN) were significantly enriched throughout the four gene classes (Figure S2A), consistent with their well-established dual roles in promoting naive pluripotency and suppressing differentiation programs (Orkin, 2005). We also identified specific Polycomb enrichment (Suz12, Mtf2) in class III and IV genes, but not in class I and II genes. This is consistent with the deposition of H3K27me3 marks at developmental regulators in EpiSCs (Gafni et al., 2013) and is also in line with reported H3K27me3 depletion (Marks et al., 2012) and the dispensability of Polycomb repression under naive 2i culture (Galonska et al., 2015). To investigate how other transcriptional cofactors and epigenetic regulators within the OSN pluripotency network (Huang and Wang, 2014) may contribute to the regulation of both naive and primed PCF transitions, we conducted RNAi screens focusing on our previously reported high-confidence OSN-interacting partners (Costa et al., 2013; Ding et al., 2012, 2015; Wang et al., 2006) (Figure S2B). These include TFs, epigenetic regulators, and RNA processing factors whose roles in pluripotent state transitions have not been explored before (Figure 2A, right). We tested whether the naive reporter (*Oct4*-ΔPE-GFP) in ESCs might be affected by depletion of these OSN partners during pluripotent state transitions (Figure 2A, left). We found that loss of several factors including the TF Zfp281 noticeably increased GFP reporter activity in all conditions tested, while the loss of other factors reduced GFP reporter activity (Figure 2A, right). Interestingly, we detected opposite effects of the ten-eleven translocation (TET) family methylcytosine hydroxylases Tet1 and Tet2, with loss of Tet1 increasing, and loss of Tet2 decreasing, *Oct4*-ΔPE-GFP activity (Figure 2A, right), respectively.

To gain insight into the molecular control of the PCF gene signature, we focused on Zfp281, a zinc-finger protein expressed in mouse ESCs, whose depletion is compatible with
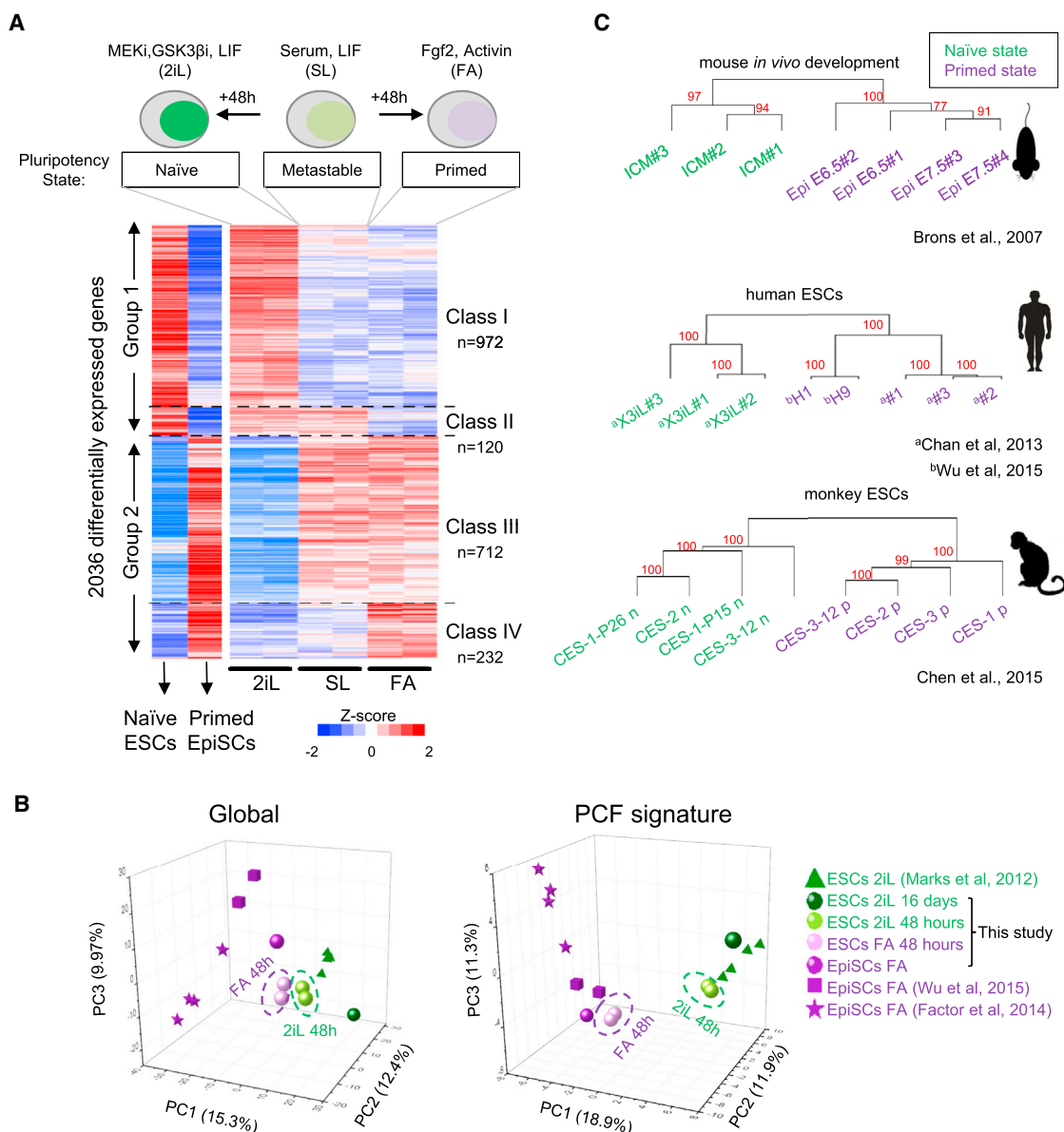
Figure 1. Identification of a Pluripotent Cell Fate Gene Signature for Alternative Pluripotency

(A) Raw normalized expression of 2,036 genes differentially expressed in SL ESCs and during transitions under 2iL or FA for 48 hr. ESCs under 2iL (naive) for 16 days and previously established EpiSCs (primed) are shown for reference. The scale represents Z score.

(B) Principle-component analysis (PCA) of transcriptome comparison between this study and published datasets. PCA was performed for the RNA-seq expression (cRPKM) data of all genes (global) or the PCF signature genes. The expression data matrix was imported by Cluster 3.0 software. Mean center and normalize genes were performed, then PCA was applied to arrays and results were virtualized using Origin software.

(C) Unbiased clustering analysis of 2,036 PCF genes across previously published transcriptomes for mouse in vivo development and human and *Cynomolgus* monkey naive and primed pluripotent cells. The approximately unbiased (AU) p value, which is computed by multiscale bootstrap resampling, is used to estimate robustness of each cluster. A cluster with AU >95% indicates that this cluster significantly exists.

See also Figure S1.

pluripotency in the SL condition (Fidalgo et al., 2011). Interestingly, Zfp281 has also been identified in a small interfering RNA (siRNA) screen as a factor required for exiting naive pluripotency (Betschinger et al., 2013) and in another study as a specific partner of Oct4 in the primed epiblast-like cell (EpiLC) state (Buecker et al., 2014). Network analyses also suggest an important role of Zfp281 in regulating the pluripotency network (MacArthur et al.,

2012). These observations together suggest that Zfp281 might be an important player in regulating the naive to primed transition. While loss of Zfp281 caused a significant enhancement of *Oct4*-ΔPE-GFP activity (Figure 2A), ectopic expression of Zfp281 confirmed the repressive role of Zfp281 on *Oct4*-ΔPE-GFP activity (Figure S2C), further suggesting that Zfp281 could be an important transcriptional regulator that promotes primed
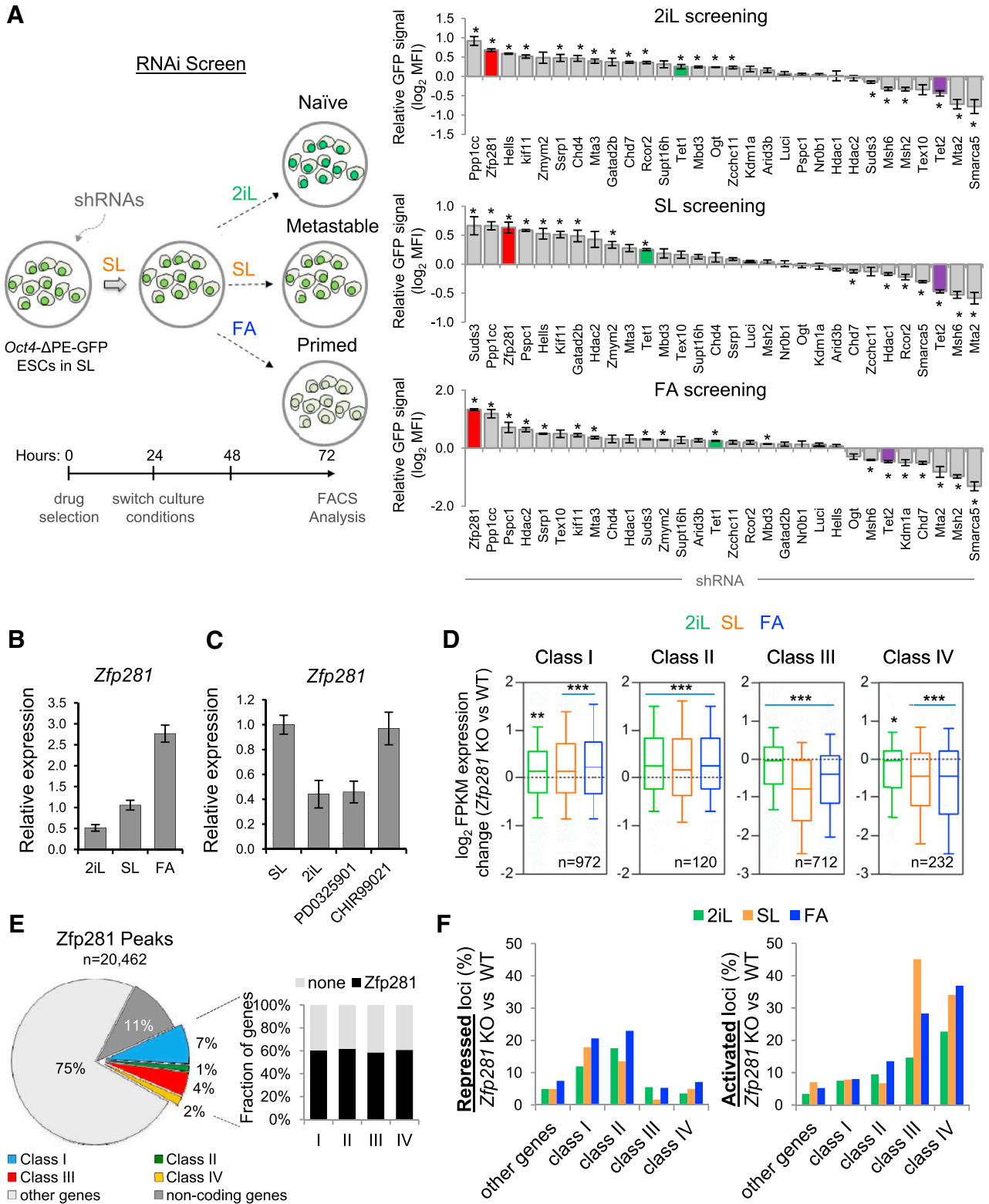
Figure 2. RNAi Screen Identifies Zfp281 as a Critical Regulator for Transcriptional Control of PCF Signature Genes

(A) A schematic overview of RNAi screen strategy (left) and results (right). *Oct4*-ΔPE-GFP reporter ESCs were infected with two independent small hairpin RNAs (shRNAs) against each candidate, and an average of mean fluorescence intensity in the cell population is measured. Error bars indicate average ± SEM (n = 2). Student's unpaired t test (*p < 0.05) relative to shRNA against luciferase (shLuci) was performed.

(legend continued on next page)

pluripotency. In agreement with this, we observed a stepwise upregulation of Zfp281 during naive to primed transition (Figure 2B) and found that Zfp281 is positively regulated by the fibroblast growth factor (FGF)-ERK signaling pathway (Figures 2C and S2D–S2G). RNA-seq analysis comparing *Zfp281* knockout (KO) ESCs to wild-type (WT) ESCs indicated significant changes in global gene expression among all four gene classes during pluripotent state transitions (Figure 2D). Notably, we found that naive active genes (classes I and II) were significantly increased, whereas primed active genes (classes III and IV) were significantly reduced upon *Zfp281* depletion (Figure 2D).

We next examined global genomic targets of Zfp281 in SL ESCs by chromatin immunoprecipitation followed by sequencing (ChIP-seq) to further investigate how Zfp281 regulates its transcriptional targets within the PCF gene signature. We identified 20,462 genome-wide peaks and found that, although all four classes of genes represent only 14% of Zfp281 binding targets, there is a pronounced binding of Zfp281 to all four gene classes (∼60% of all targets within each class of genes) (Figure 2E). Using unbiased hierarchical clustering and published ChIP-seq datasets of histone marks, we detected a striking correlation between Zfp281 and epigenetic marks associated with transcriptional regulation (Figure S2H). The presence of both activating and repressive histone marks on PCF signature gene loci suggests that Zfp281 may mediate both transcriptional activation and repression. Consistent with this, analysis of gene expression changes in *Zfp281* KO relative to WT cells and Zfp281 occupancy confirmed a predominantly repressive and activating function of Zfp281 at naive (classes I and II) and primed (classes III and IV) genes, respectively, across the three pluripotent states (Figures 2F and S2I–S2K).

Taken together, our data indicate that Zfp281 is a critical regulator for the PCF signature gene expression with dual functions in transcriptional activation and repression of primed and naive genes, respectively.

Zfp281 Is Required for Establishment and Maintenance of Primed Pluripotency

To directly test the function of Zfp281 in the pluripotent state transition, we cultured *Zfp281* WT and KO ESCs in defined media and found that *Zfp281* KO ESCs could not be maintained in the FA culture condition for more than three passages, whereas no significant proliferation differences were found in 2iL or SL conditions (Figure 3A). We next examined whether self-renewal properties of each specific pluripotent state were affected by the absence of Zfp281. Colony-formation assays indicated that *Zfp281* KO ESCs yielded significantly more naive compact dome-shaped colony numbers under all culture conditions (Figure 3B). Remarkably, the typical primed diffuse-shaped colonies

as well as expression of lineage-primed markers were severely compromised by Zfp281 depletion during primed transition (Figure S3A), demonstrating that *Zfp281* KO promotes naive pluripotency, as evident by increased Nanog expression in the primed culture condition (Figure 3C). Conversely, we found that ectopic Zfp281 expression was sufficient to promote primed features, including flattened colony morphology and downregulation of naive and upregulation of primed pluripotency markers, in SL ESCs and during the SL to FA transition (Figure S3B). Furthermore, we found that EpiSCs could not be stably maintained in the primed state upon Zfp281 knockdown due to compromised proliferation, elongated G1 phase, and increased cell death (Figures 3D and S3C–S3F). Within 6 days upon Zfp281 depletion, EpiSCs upregulate naive markers (*Nanog*, *Prdm14*, *Esrrb*, and *Nr0b1*) and downregulate primed makers (*Fgf5*, *Otx2*, *Brachyury*, and *Eomes*) (Figures S3G and S3H). These loss-of-function defects can be rescued by transgenic Zfp281 re-expression ("+R"; Figures 3D and S3C–S3H). Together, our data clearly demonstrate that Zfp281 functions as a key factor that is critical for both induction and maintenance of primed pluripotency. While EpiSCs undergo massive cell death during the transition to the naive state under 2iL as previously reported (Guo et al., 2009), when cultured in 2iL immediately following Zfp281 knockdown, EpiSCs showed significant enhancement of reprogramming efficiency toward the naive state (Figure 3E). We confirmed bona fide naive pluripotency of the resulting Epi-iPSCs by their contribution to the germ lineage as well as chimeric embryos after blastocyst injection (Figure 3F). These data suggest that Zfp281 functions as a major barrier for primed to naive reversion.

Conventional human ESCs (hESCs) are also considered to be in a primed pluripotent state. As the PCF gene signature is conserved in humans (Figure 1C), we also tested whether the human ortholog ZNF281 plays similar roles in maintaining the primed pluripotency of hESCs and whether it also poses as a barrier in converting primed hESCs to a naive state. Using hESCs harboring an OCT4-2A-GFP reporter (O4G) (Hockemeyer et al., 2011), we found that ZNF281 knockdown compromised self-renewal of these hESCs under conventional culture conditions as shown by smaller GFP-positive and AP-positive colonies (Figure 3G). Nonetheless, these small colonies became less flattened and maintained (e.g., *OCT4* and *PRDM14*) or even upregulated (e.g., *KLF2/4/5*, *DPPA3/5*, *TCFP2L1*, and *TET2*) naive pluripotency marker gene expression (Figures S3I and S3J). When switching the culture conditions from conventional medium to the defined naive medium containing five small-molecule inhibitors and LIF (5iL) (Theunissen et al., 2014), we observed a dramatic increase in the number of naive AP-positive (Figures 3H and 3I) and GFP-positive (Figure S3K) hESCs using two independent GFP reporter lines upon ZNF281 depletion. Together,

(B) Relative expression of Zfp281 analyzed by qPCR during pluripotent state transitions after 48 hr medium switch as indicated.

(C) Relative expression of Zfp281 by qPCR in SL ESCs under treatment of the MEK and GSKβ inhibitors. Note that Zfp281 is downregulated by the MEK inhibitor (PD0325901), but not the GSKβ inhibitor (CHIR99021).

(D) Expression changes of PCF gene classes in SL and under 48-hr transition to 2iL and FA in *Zfp281* KO relative to WT cells (mRNA-seq, two biological replicates per condition). Whiskers extend to the 10th–90th percentile range. p values between KO and WT ESCs were calculated using a one-sided Wilcoxon signed rank test (***p < 0.0001, **p < 0.001, *p < 0.01). n indicates number of genes analyzed per gene class.

(E) Distribution of total Zfp281 binding peaks (left), and percentages of PCF gene class occupancy by Zfp281 (right).

(F) Transcriptional effects of Zfp281 in target loci. Percentages of repressed and activated loci were calculated by comparative gene expression changes between *Zfp281* KO cells and WT cells (>2-fold differences).
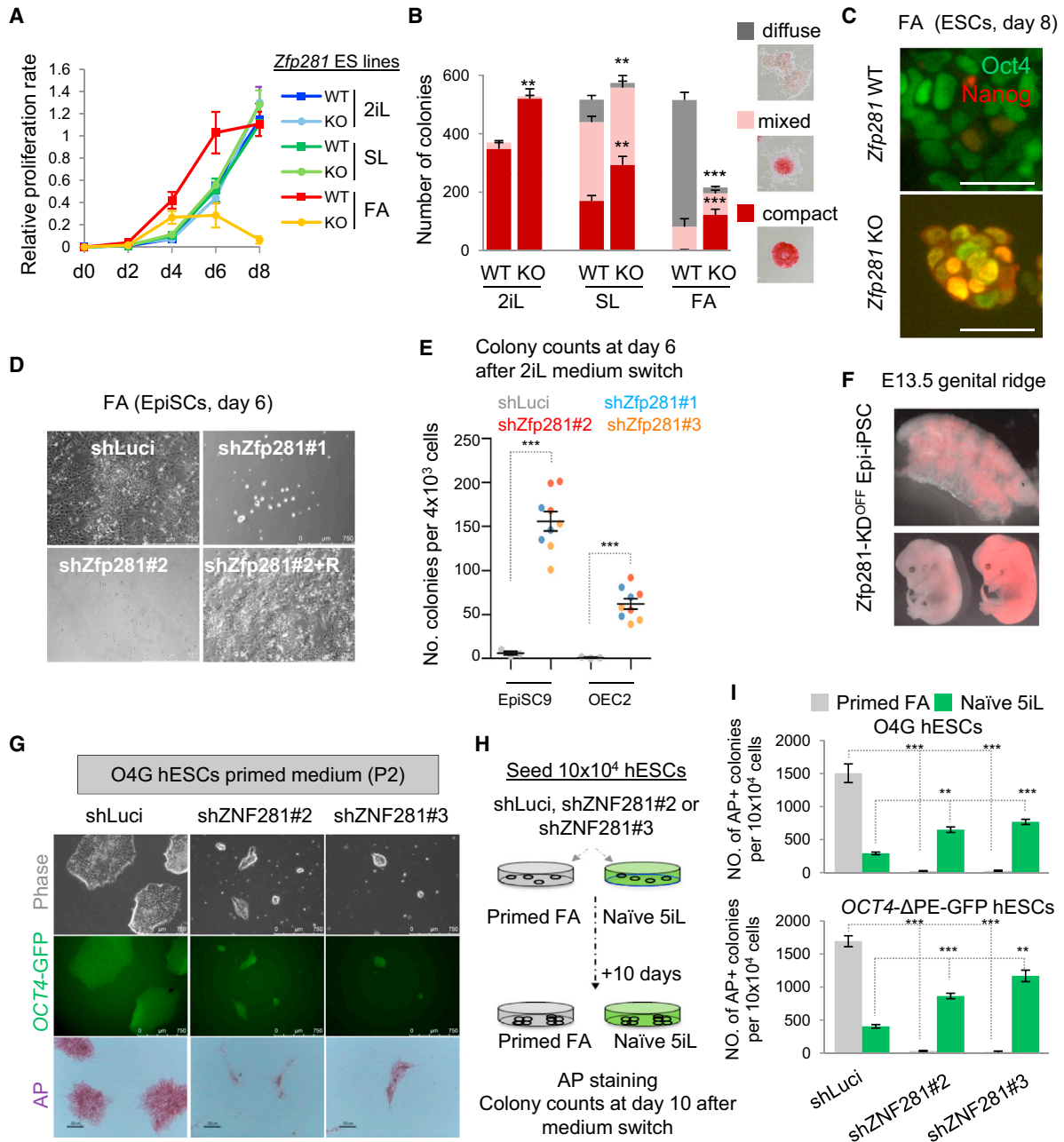
See also Figure S2.

Figure 3. Zfp281 Is Critical for Primed Pluripotency

(A) Proliferation analysis of WT and *Zfp281* KO ESCs cultured in SL, 2iL, or FA. Error bars indicate average ± SEM (n = 3).

(B) Colony-formation assay for WT and *Zfp281* KO ESCs. Colonies were stained for alkaline phosphatase (AP) activity at day 6 of culture in specified conditions, and positive colonies were scored into three categories (compact, mixed, and diffuse as indicated). Error bars indicate average ± SEM (n = 6). Student's unpaired t test (***p < 0.001, **p < 0.01) relative to WT ESCs was performed.

(C) Immunostaining of Nanog and Oct4 at day 8 under FA. Scale bars represent 100 μm.

(D) Representative bright-field images at day 6 of Zfp281 KD (shZfp281) EpiSCs and rescued (+R) line compared with control *luciferase* knockdown (shLuci) EpiSCs.

(E) Zfp281 KD facilitates reprogramming of EpiSCs toward naive-like cells (Epi-iPSCs). Two different EpiSC lines were transfected with three independent shRNAs against Zfp281, and Epi-iPSC colony numbers were quantified at day 6 in 2iL. Error bars indicate average ± SEM (n = 3). Student's unpaired t test (***p < 0.001) relative to shLuci was performed.

(F) Contribution of Epi-iPSCs to the germline (top) and chimeric E13.5 mouse embryos (bottom). Epi-iPSCs were generated by reprogramming EpiSCs with pTRIPZ-shZfp281. Epi-iPSCs were labeled with a Tomato reporter transgene and maintained without Dox (OFF).

(G) ZNF281 dependency of conventional hESCs. Representative colony morphology under bright-field (top) and fluorescent (for *OCT4*-GFP; middle) microscope as well as AP-stained colonies (bottom) is shown. ZNF281-depleted and control shLuci O4G hESCs were passaged twice in primed culture conditions before microscopy.

(legend continued on next page)

these results establish Zfp281/ZNF281 as a key primed pluripotency regulator in both mouse and human ESCs, with its depletion promoting naive pluripotency.

Zfp281 Functions in Epigenomic Reconfiguration during Pluripotent State Transitions

To explore the molecular mechanisms by which Zfp281 regulates PCF signature gene expression during pluripotent state transitions, we performed affinity purification of Zfp281 protein complexes followed by mass spectrometry (AP-MS) in SL ESCs and identified 196 high-confidence Zfp281-interacting partners (Figure 4A; Table S4). GO analysis of the Zfp281 interactome revealed a significant association of Zfp281 with chromatin regulatory functions due to the presence of many histone- and DNA-modifying enzymes, including Tet1, HDAC-containing NuRD and Sin3a complexes, MLL complex, and Polycomb complex proteins (Figures 4A and 4B). In accord with this, global alterations of certain histone modifications (e.g., increased H3K27ac under SL and FA) with corresponding histone code reader/writer changes (e.g., reduced chromatin bound HDAC2 under SL and FA) upon Zfp281 depletion were observed (Figures S4A and S4B). As DNA hypomethylation is a prominent feature of naive pluripotency (Marks et al., 2012) and developmental progression from naive to primed cell fate is intrinsically associated with DNA methylation (Clark, 2015), we decided to address how Zfp281 may contribute to this important epigenomic reconfiguration in pluripotent state transitions by assaying global alterations of 5mC and 5hmC levels in Zfp281 WT and KO ESCs. Quantitative immunofluorescence analysis of single cells and dot-blot analysis revealed a significant reduction of 5mC and increase of 5hmC upon Zfp281 depletion under the three pluripotent states (Figures 4C, S4C, and S4D).

Analysis of global target binding of Zfp281 and many pluripotency TFs and epigenetic regulators revealed a strong correlation in genome-wide occupancy between Zfp281 and Tet1/2 (Figure 4D), prompting us to test whether active DNA demethylation via Tet-mediated 5hmC may contribute to the transcriptional regulatory functions of Zfp281 during pluripotent state transitions. We therefore compared the global transcriptional profiles of Zfp281 KO and Tet1/2/3 triple-knockout (Tet-TKO) ESCs (Dawlaty et al., 2014). While we observed that global deregulation (>2-fold expression change) of 830 shared genes in both Zfp281 KO and Tet-TKO cells represents only 26.05% of the total misregulated genes in the absence of Tet proteins, a significantly higher proportion (57.51%) of misregulated genes in Tet-TKO cells was shared with Zfp281 KO cells when only the PCF signature genes were compared (Figure 4E), highlighting a potential functional relationship between Zfp281 and Tet proteins in regulating PCF signature genes. Interestingly, the majority of 268 identified shared PCF genes showed opposite expression changes in Zfp281 KO versus Tet-TKO ESCs (Figure 4F). The significant upregulation of 5hmC in Zfp281 KO ESCs (Figure 4C) suggests potentially activated Tet functions upon Zfp281 depletion as the most parsimonious explanation. Together with the

physical association between Zfp281 and Tet1, but not Tet2 (Figure 4A), our data indicate a complex interplay among Tet1, Tet2, and Zfp281 in transcriptional and epigenetic control of PCF signature gene expression during pluripotent state transitions.

Tet2 Is Regulated at the Transcriptional and Post-transcriptional Levels by Zfp281

To explore which Tet protein might be activated upon Zfp281 depletion, we examined our RNA-seq data and found that Tet2, but not Tet1, is significantly upregulated in Zfp281 KO ESCs (Figure S5A), and this was validated by qPCR (Figure 5A). We also found three ChIP-seq peaks of Zfp281 binding to the regulatory regions of the Tet2 locus bearing enhancer marks (Figure S5B). Because histone deacetylase (HDAC) complexes are present in the Zfp281 interactome (Figure 4A), and because depletion of Zfp281 also increases global H3K27ac levels (Figure S4A), we asked whether Zfp281 might modulate histone acetylation levels at the Tet2 enhancer. Indeed, we found that loss of Zfp281 reduced binding of HDAC2 with a concomitant increase in H3K27ac enrichment at the Tet2 enhancer (Figures 5B and 5C), indicating that Zfp281 may regulate Tet2 enhancer activity through modulating histone acetylation. In line with this, we found that Tet2 was upregulated upon knockdown of HDAC proteins, especially HDAC2 (Figure S5C). In addition, chemical inhibition of HDACs with valproic acid (VPA) increased Tet2 expression in WT ESCs but was unable to promote further upregulation of Tet2 in Zfp281 KO ESCs (Figure 5D), suggestive of Zfp281-dependent action of HDACs on the Tet2 enhancer. Interestingly, we detected a lower level of Tet2 in WT ESCs treated with VPA than that in Zfp281 KO ESCs regardless of VPA treatment, suggesting that Zfp281 must also regulate Tet2 beyond the transcriptional level.

To investigate whether and how Zfp281 may participate in the regulation of Tet2 levels in a post-transcriptional manner, we first examined the presence of Zfp281 in non-coding gene regions (Figure 2E) and found the enrichment of a significant fraction of microRNAs (miRNAs) (Figure S5D). We therefore performed global mature miRNA expression profiling in Zfp281 WT and KO ESCs and identified candidate miRNAs that are regulated by Zfp281 (Figure S5E). We hypothesized that miRNAs that are positively regulated by Zfp281 would be the candidates to directly target Tet2 mRNA for repression. Among them, we focused our interest on the miR-302/367 cluster (Figure S5F), because (1) only Tet2, but not Tet1, is a predicted target of miR-302/367 (Figure 5E); (2) the presence of this mature miRNA family is greatly diminished in the absence of Zfp281 (Figure 5F); and (3) the expression of this pluripotency miRNA family shows the opposite trend to that of Tet2 expression during pluripotent state transitions (compare Figure 5A with Figure 5G). qPCR analysis confirmed that Zfp281 is required for transcriptional activation of pri-miRNA-302/367 (Figures 5G and S5G). We next tested whether this miRNA cluster participates in the post-transcriptional regulation of Tet2 in ESCs and found that enforced expression of this miRNA cluster in SL ESCs downregulated Tet2, whereas its inhibition in FA cells led to a

(H) A strategy to test effects of ZNF281 depletion on converting primed hESCs to a naive state using the published 5iL condition.

(I) Quantification of AP-positive colony numbers of hESCs at day 10 of primed human embryonic stem (ES) medium (FA) or naive culture conditions (5iL) upon control or ZNF281 KD. Error bars indicate average ± SEM (n = 3). Student's unpaired t test (***p < 0.001, **p < 0.01) relative to shLuci hESCs.
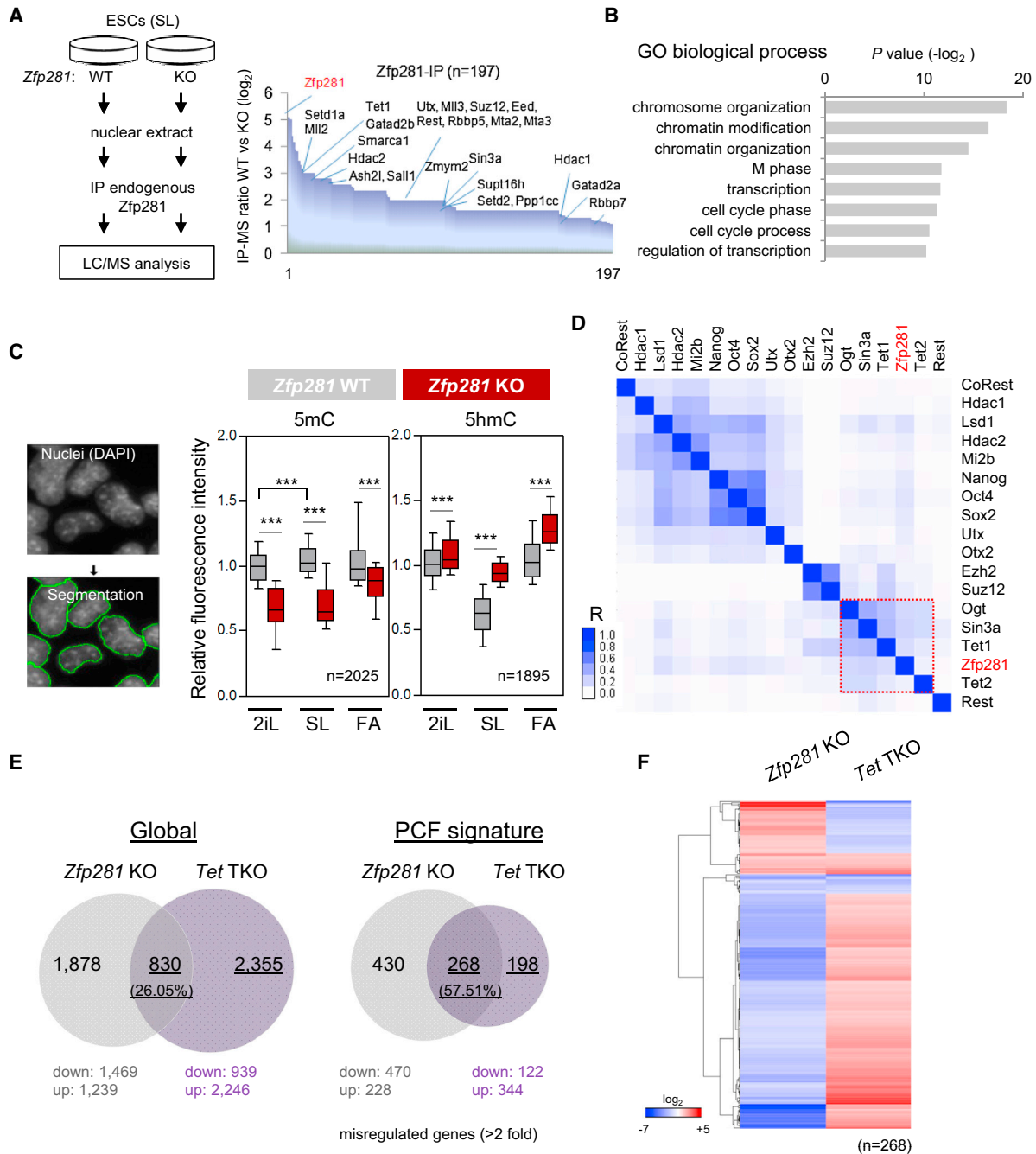
See also Figure S3.

Figure 4. Characterization of Epigenetic Reconfiguration Dynamics in *Zfp281* KO ESCs

(A) Affinity purification and mass spectrometry (AP-MS) identification of Zfp281-interacting partners. Depiction of Zfp281 antibody-based AP-MS procedure (left), and candidate partners (n = 197) ordered by fold change in peptide numbers between *Zfp281* WT and KO ESCs (right panel). Chromatin modifiers are shown.

(B) Gene Ontology (GO) analysis for biological processes associated with Zfp281-interacting partners identified by AP-MS.

(C) Global decrease of 5mC is accompanied by an increase of 5hmC upon *Zfp281* depletion. Single-cell quantitative immunofluorescence was performed in *Zfp281* WT and KO cells cultured in SL and after 48 hr of medium switch to 2iL or FA. Signals were normalized against DAPI nuclei staining. Whiskers extend to the 10th–90th percentile range. p values between KO and WT ESCs were calculated using a one-sided Wilcoxon signed rank test (***p < 0.0001). "n" indicates number of cells analyzed per condition.

(D) Hierarchical clustering of Zfp281 and chromatin associated factors in genome-wide occupancy. The scale represents a Pearson correlation coefficient (R), and the red rectangle indicates a group of factors with a high correlation.

(E) Pairwise comparisons of the number of genes misregulated (>2-fold alteration compared to WT cells) in *Zfp281* KO and *Tet* triple-knockout (*Tet*-TKO) ESCs under SL culture.

(F) Relative expression of 268 misregulated genes in *Zfp281* KO cells compared with *Tet*-TKO cells. The scale represents fold changes compared to WT cells. See also Figure S4.
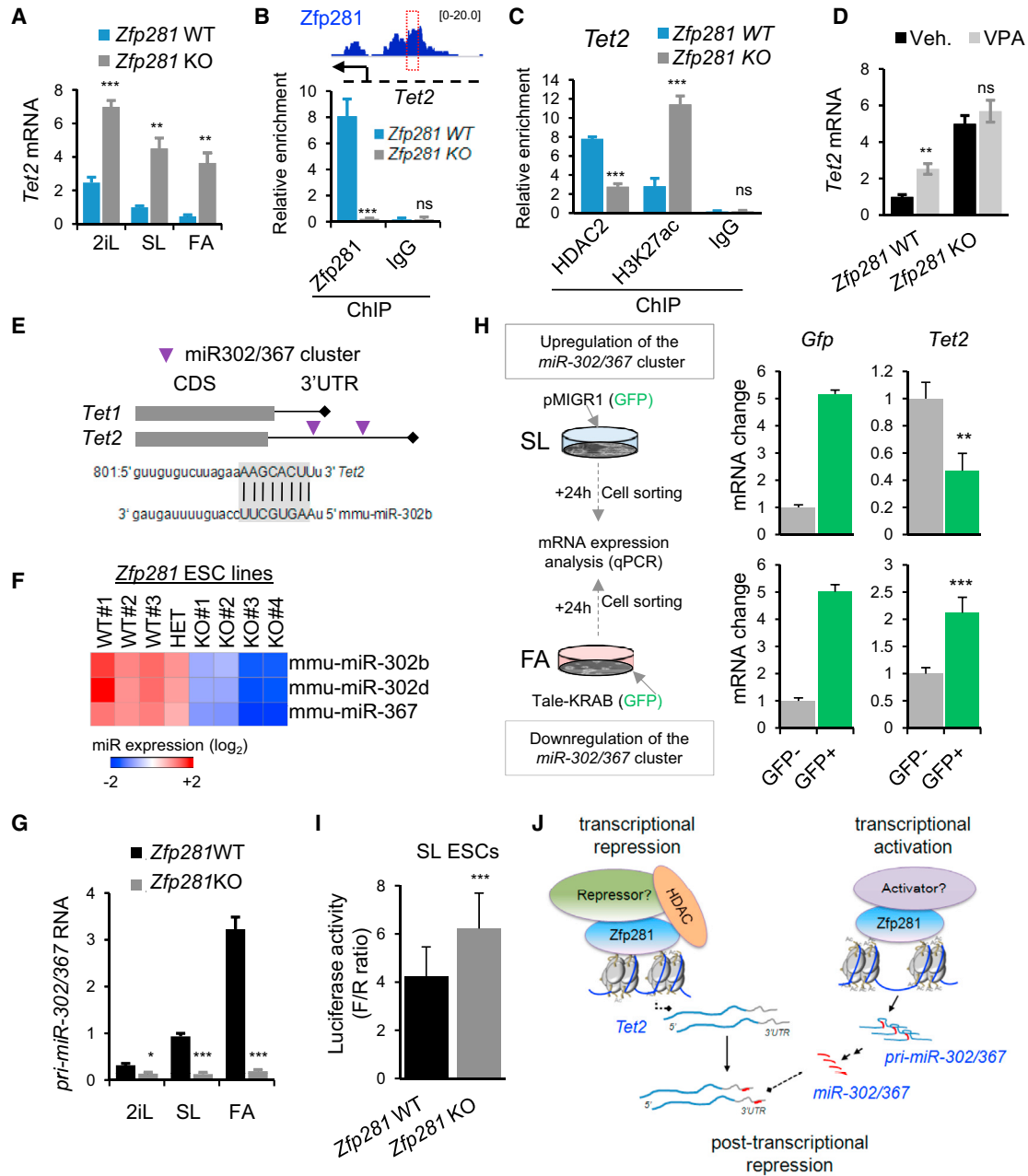
Figure 5. Transcriptional and Post-transcriptional Regulation of Tet2 by Zfp281

(A) Relative expression of *Tet2* by qPCR showing upregulation of *Tet2* in *Zfp281* KO relative to WT ESCs cultured during 48-hr pluripotent state transitions.

(B) Enrichment of Zfp281 at the regulatory locus of *Tet2* by ChIP-qPCR validating *Tet2* as a direct transcriptional target of Zfp281.

(C) ChIP-qPCR analysis of relative enrichment of HDAC2 and H3K27ac at the Zfp281 binding *Tet2* loci as indicated in (B).

(D) Chemical inhibition of HDAC activity increases Tet2 expression in *Zfp281* WT, but not KO cells. Expression analysis was determined by qPCR in *Zfp281* KO and WT ESCs treated with VPA (0.5 mM) for 24 hr.

(E) Schematic depiction of seed sequences for miR-302/367 cluster on *Tet1* and *Tet2* genes. Seed match sequences of miR-302b within *Tet2* 3′ UTR were shown.

(F) Relative expression of mature miR-302b, miR-302d, and miR-367 detected by an miRCURY LNA Array in *Zfp281* WT, HET (heterozygous), and KO ESCs. The color scale bar represents fold change.

(G) Relative expression of pri-miR-302/367 cluster measured by qPCR in *Zfp281* KO and WT ESCs at SL and 48 hr at 2iL or FA.

(H) Depiction of miR-302/367 cluster gain- and loss-of-function assays (left), and qPCR analysis of *Tet2* expression levels (right).

(I) Zfp281 depletion enhances firefly luciferase activity. *Zfp281* KO and WT ESCs were transiently transfected with the luciferase reporter tethering to the 3′-UTR of *Tet2*. Renilla reporter was included for normalization (F/R ratio).

(J) A model illustrating the transcriptional activation and repression roles of Zfp281 in regulating *Tet2* expression.

All error bars in this figure indicate average ± SEM (n = 3). p values were determined by Student's unpaired t test (ns, not significant; ***p < 0.0001, **p < 0.001).
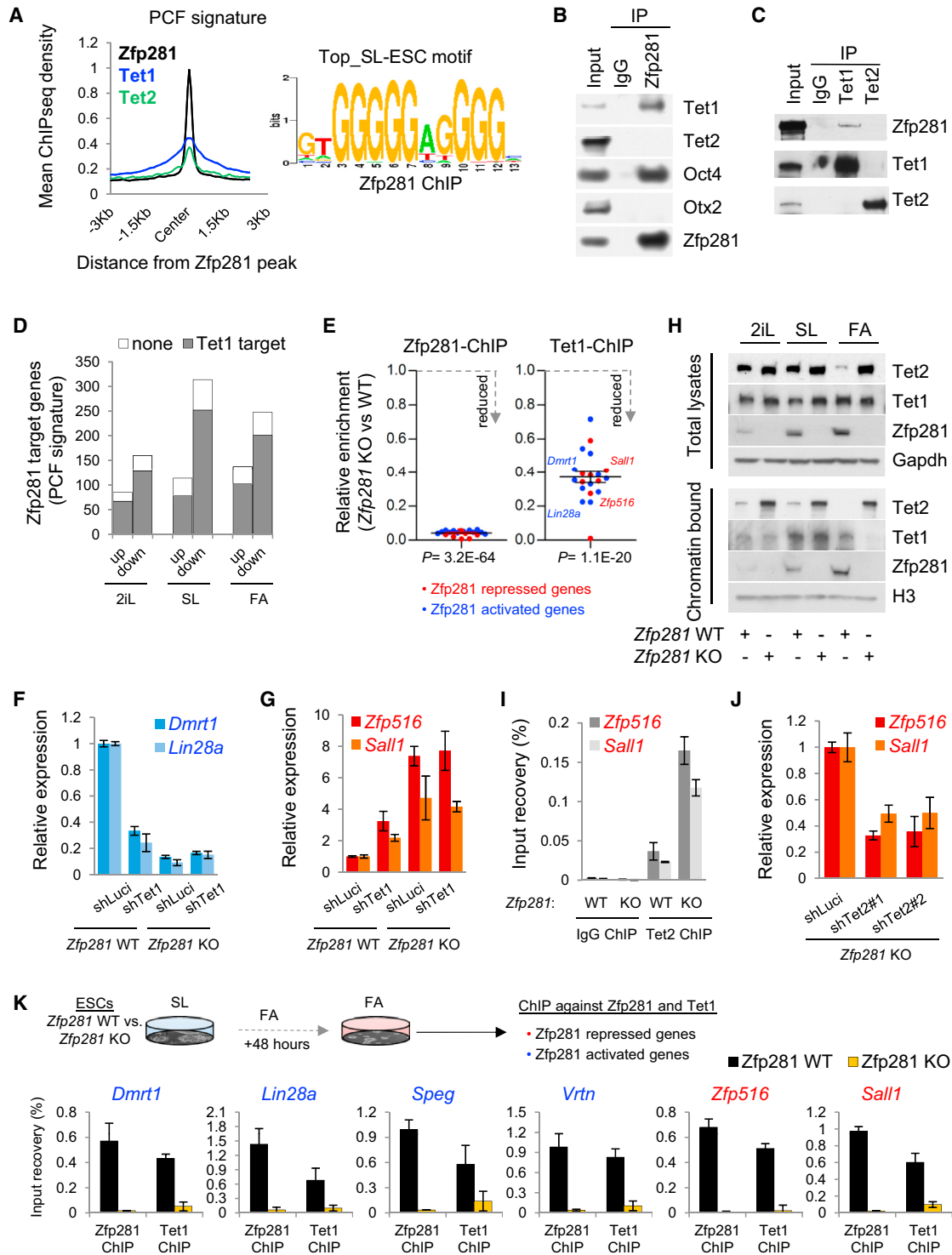See also Figure S5.

Figure 6. Distinct Functions of Tet1 and Tet2 in Modulating Zfp281-Mediated Transcriptional Control

(A) Average ChIP-seq read density of Zfp281, Tet1, and Tet2 near the Zfp281 peak center on PCF genes (left) and the top Zfp281 binding motif in SL ESCs (right).

(B) Zfp281 interacts with Tet1 and Oct4, but not Tet2 or Otx2, in SL ESCs. Immunoprecipitation (IP) was performed using anti-Zfp281 antibody followed by western blotting with indicated antibodies.

(C) Zfp281 interacts with Tet1, but not Tet2, in SL ESCs. IP was performed using anti-Tet1 and anti-Tet2 antibodies followed by western blotting with indicated antibodies.

(D) Comparison of Zfp281-regulated PCF gene targets with Tet1 targets showing the majority of Zfp281-regulated PCF target genes that are misregulated in *Zfp281* KO ESCs are also Tet1 targets during pluripotent state transitions.

(legend continued on next page)

significant upregulation of *Tet2* (Figure 5H). We further confirmed this potential post-transcriptional regulation of *Tet2* expression by Zfp281-controlled *miR-302/367* using a luciferase reporter tethering to the *Tet2* 3′ UTR, which contains the *miR-302/367* seed sequences. Our data show increased luciferase activity in *Zfp281* KO relative to WT ESCs (Figure 5I) and an inverse expression pattern between luciferase activity/Tet2 and Zfp281/pri-miR-302/367 under the three pluripotent states (Figure S5H).

Collectively, our data establish Zfp281 as a major regulator of *Tet2* expression in pluripotency control by direct transcriptional repression through histone deacetylation of the *Tet2* enhancer and indirect post-transcriptional repression through activation of *miR-302/367* (Figure 5J).

Distinct Functions of Tet1 and Tet2 in Zfp281-Mediated Transcriptional Control of Naive to Primed Transition

To understand how Tet1 and Tet2 contribute to transcriptional regulatory functions of Zfp281, we compared our Zfp281 ChIP-seq data (Figure 2E) with genomic occupancy of Tet1 (Wu et al., 2011) and Tet2 (Chen et al., 2013) under the same SL conditions. We found that Zfp281 has a significant overlap with Tet1 and Tet2 in controlling specific PCF signature gene occupancy (Figures 6A and S6A). Remarkably, 81.8% of the signature genes (505 out of 617) that are bound by Zfp281 and misregulated in *Zfp281* KO ESCs are also directly bound by at least one Tet protein (predominantly Tet1) (Figure S6B), strongly suggesting that Tet proteins are required for proper transcriptional regulation of Zfp281 target genes. Moreover, expression analysis of these 505 misregulated genes indicated that they were subjected to both transcriptional activation and repression in all pluripotent states (Figure S6C), consistent with the dual functions of Tet1 in transcriptional regulation in mouse ESCs (Wu et al., 2011).

The identification of Tet1, but not Tet2, as a partner of Zfp281 in SL ESCs (Figure 4A), and the marked reduction of Tet2 expression from naive to primed transition (Figure S6D), prompted us to consider whether Tet1 might be the critical Tet family member for modulating Zfp281 transcriptional regulatory functions during the transition. We confirmed the physical interaction between Zfp281 and Tet1, but not Tet2, in SL ESCs (Figures 6B and 6C). We also observed the majority of Zfp281 direct targets within the PCF signature that are misregulated upon Zfp281 depletion being also Tet1 targets during the transitions (Figure 6D). ChIP-qPCR experiments showed that loss of Zfp281 reduced Tet1 binding to several common targets that are either repressed (e.g., *Zfp516* and *Sall1*) or activated (e.g., *Dmrt1* and *Lin28a*) by Zfp281 in ESCs during pluripotent state transitions (Figures 6E and S6C). More importantly, we detected reduced 5hmC levels at targets that are downregulated in the absence of Zfp281 (e.g., *Lin28a*) during the pluripotent state transitions (Figure S6E).

These data suggest that Zfp281 may recruit Tet1 to a subset of shared target genes to promote transcriptional activation through 5hmC deposition during the transitions. This Zfp281-dependent transcriptional activation function of Tet1 was confirmed by downregulation of *Dmrt1* and *Lin28a* upon *Tet1* knockdown in WT, but not in *Zfp281* KO, ESCs (Figure 6F). In contrast, we detected increased 5hmC levels at several shared target genes (e.g., *Zfp516* and *Sall1*) (Figure S6E) that showed significant upregulation in the absence of Zfp281 (Figures 6G and S6C). This result is quite surprising, as chromatin-bound Tet1 is greatly diminished upon Zfp281 depletion in FA cells despite the presence of similar amounts of total Tet1 proteins (Figure 6H), which prompted us to examine the effect of *Zfp281* KO on total and chromatin-bound protein levels of Tet2. In agreement with the repressive role of Zfp281 on Tet2 expression (Figure 5), we found that loss of Zfp281 increased the protein levels of both total and chromatin-bound Tet2 during transitions, whereas the levels of chromatin-bound Tet1 were only affected (i.e., reduced) in FA culture (Figure 6H). These results suggest that Tet2 may be responsible for the elevated 5hmC levels observed in the absence of Zfp281, leading to transcriptional activation. We confirmed that *Zfp281* KO increased Tet2 binding to the regulatory loci of upregulated genes *Zfp516* and *Sall1* (Figure 6I). Conversely, we observed decreased expression of both genes after *Tet2* knockdown in *Zfp281* KO ESCs (Figure 6J). Thus, we established a role for Tet2 in contributing to transcriptional activation of genes that are upregulated upon Zfp281 depletion. Interestingly, a Zfp281-dependent repressive role of Tet1 was also observed for *Zfp516* and *Sall1* expression, as shown by their upregulation upon Tet1 knockdown in WT, but not in *Zfp281* KO, cells (Figure 6G). We further confirmed the recruitment of Tet1 to the chromatin by Zfp281, but not the other way around, for transcriptional activation and repression by Zfp281 and Tet1 (Figures S6F and S6G). Such an effect is less obvious under 2iL due to the already low Zfp281 expression in naive cells but becomes more pronounced in SL, and particularly in FA conditions (Figure 6K), where Zfp281 is highly abundant and plays a major role as a key primed pluripotency factor.

Together, our results reveal Zfp281-coordinated distinct functions of Tet1 and Tet2 in transcriptional control of the PCF gene signature during naive and primed transitions.

Tet1 and Tet2 Play Opposing Roles in Regulating Primed and Naive Pluripotent States

In support of their distinct functions in PCF gene regulation during pluripotent state transitions described above, we found that ectopic expression of Tet2, but not Tet1, was sufficient to promote naive features (i.e., dome-shaped colony formation and increased clonogenicity) in primed culture conditions

---

(E) Validation of Zfp281-dependent Tet1 binding to the target genes by ChIP-qPCR. Error bars indicate average ± SEM (n = 20). p values were determined by Student's unpaired t test.

(F) Zfp281-dependent transcriptional activation function of Tet1. Error bars indicate average ± SEM (n = 3).

(G) Zfp281-dependent transcriptional repression function of Tet1. Error bars indicate average ± SEM (n = 3).

(H) Western blot analysis of total and chromatin-bound Zfp281, Tet1, and Tet2 levels in *Zfp281* WT and KO cells cultured in SL, 2iL, or FA for 48 hr.

(I) Analysis of Tet2 enrichment at the Zfp281 repressed loci (*Zfp516* and *Sall1*) in the presence (WT) and absence (KO) of Zfp281 in SL ESCs. Error bars indicate average ± SEM (n = 3).

(J) Knockdown of Tet2 partially rescues *Zfp516* and *Sall1* upregulation in Zfp281 KO ESCs under SL culture condition. Error bars indicate average ± SEM (n = 3).

(K) Zfp281-dependent binding of Tet1 to the candidate target genes under the FA condition by ChIP-qPCR.
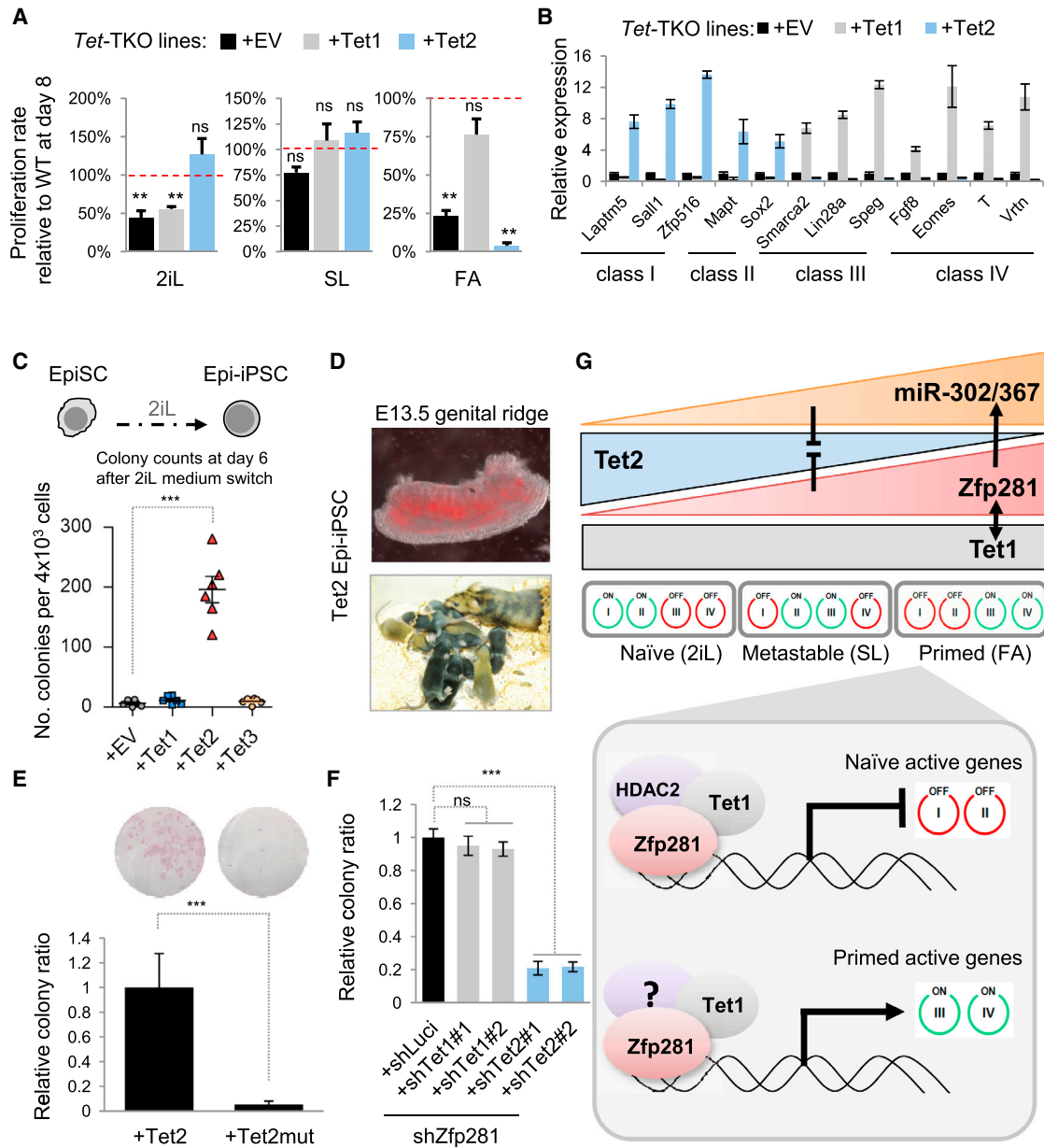
See also Figure S6.

Figure 7. Opposing Functions of Tet1 and Tet2 in Primed and Naive Pluripotent State Transitions

(A) Pluripotent state transition test of *Tet*-TKO ESCs rescued with empty vector (EV), Tet1, or Tet2 and cultured in SL, 2iL, and FA for 8 days. Proliferation rates of rescued *Tet*-TKO cells relative to WT cells (100%) were presented. Error bars indicate average ± SEM (n = 3). Student's unpaired t test was performed (ns, not significant; **p < 0.01).

(B) qPCR analysis for naive (class I/II) and primed (class III/IV) marker expression in indicated transgenic lines under SL culture conditions. Error bars indicate average ± SEM (n = 3).

(C) Ectopic expression of Tet2 promotes EpiSC reprogramming to a naive state. Quantification of the Epi-iPSC colony numbers was shown at day 6 of 2iL treatment.

(D) Contribution of Tet2 Epi-iPSCs (labeled with a Tomato reporter transgene) to the germline at E13.5 (top) and live-born chimeras (bottom) after blastocyst injection.

(E) Ectopic expression of a catalytic activity deficient Tet2 mutant (Tet2Mut) fails to reprogram EpiSCs. Representative images of alkaline phosphatase (AP) staining are also shown.

(F) Knockdown of Tet2, but not Tet1, compromises efficient EpiSC reprogramming mediated by Zfp281 depletion. EpiSC reprogramming was performed under the combinatorial KDs as indicated. All error bars in the reprogramming assays indicate average ± SEM (n = 3). Student's unpaired t test was performed (ns, not significant; ***p < 0.001).

(G) A model for Zfp281 functions in coordinating opposing functions of Tet1 and Tet2 for primed and naive pluripotency. (Top) The relative expression of Tet1/2, Zfp281, and PCF gene classes during pluripotent state transitions. (Bottom) In the primed pluripotent state, Zfp281 recruits Tet1 and HDAC-containing

(legend continued on next page)

(Figures S7A and S7B). Additionally, we found that the ability of Tet2 to promote naive pluripotency is dependent on its catalytic activity, as ectopic expression of a catalytic activity deficient Tet2 mutant (Tet2Mut) abolished the ability of this enzyme to promote naive pluripotency (Figures S7A and S7B). To conclusively establish a pluripotent-state-specific function of Tet1 and Tet2, we employed *Tet*-TKO ESCs, which self-renew normally in SL culture, and introduced individual Tet1 or Tet2 (and Tet2Mut) for transgenic rescue (Figure S7C), followed by the pluripotent state transition test. We found that *Tet*-TKO cells are defective in transitioning to either the naive or primed pluripotent state (Figure 7A, black bars), supporting that Tet functions are important in regulating alternative pluripotent states. Our finding that Tet1 is critical for primed and Tet2 for naive pluripotency was substantiated by efficient transition to primed pluripotency and inhibition of naive pluripotency upon Tet1 rescue (Figure 7A, gray bars) and by efficient transition to naive pluripotency but inhibition of primed pluripotency upon Tet2 rescue (Figure 7A, blue bars). Such a critical role of Tet2 in promoting naive pluripotency while inhibiting primed pluripotency is dependent on its catalytic activity (Figure S7D) and is manifested with rescued cells under FA for 6 days still expressing highly abundant Nanog (Figure S7E). Accordingly, we found that Tet2 promoted the upregulation of naive active class I/II genes and the repression of primed active class III/IV genes, whereas opposite effects on the same genes were detected upon rescue with Tet1 (Figure 7B).

To further investigate the opposing functions of Tet1/2 proteins in regulating primed and naive pluripotent states, we examined how individual Tet proteins might affect the reprogramming of primed EpiSCs to a naive state. Remarkably, we found that Tet2 alone, but not Tet1 or Tet3, was able to facilitate the reprogramming of EpiSCs to naive Epi-iPSCs under 2iL condition (Figure 7C), supporting the naive specific function of Tet2. Germline contribution and live-born chimeras after blastocyst injection confirmed the pluripotency status of these Epi-iPSCs (Figure 7D). In contrast, Tet2Mut failed to promote EpiSC reprogramming to a naive state (Figure 7E). Because endogenous *Tet2* was not detectable in EpiSCs (Figure S7F) and upregulated at both protein and RNA levels upon Zfp281 knockdown (Figures S7G and S7H), and because we detected increased 5hmC levels at naive loci in *Zfp281*-knockdown EpiSCs (Figure S7I), we tested whether knockdown of *Tet2* could abrogate the reprogramming effect of Zfp281 depletion. In agreement with our observations, downregulation of Tet2, but not Tet1, led to a significant reduction in the 5hmC levels at naive pluripotency gene loci (Figure S7I) and compromised reprogramming efficiency of *Zfp281* KD EpiSCs (Figure 7F). Taken together, our data establish primed and naive pluripotent-state-specific functions of Tet1 and Tet2, respectively, in regulating pluripotency.

DISCUSSION

We have established a unique PCF gene signature that is evolutionarily conserved in distinguishing the naive from the primed pluripotent state. Investigation into the upstream regulators of the PCF gene expression signature underlying genetically identical and homogeneous naive and primed pluripotent cell populations led us to the discovery of Zfp281 as a key transcriptional regulator for primed pluripotency as well as opposing functions of the DNA hydroxylases Tet1 and Tet2 in regulating primed and naive pluripotent states, respectively. Our study demonstrates an important contribution of Tet2 to the epigenetic reprogramming of primed pluripotency to a naive state, whereas Tet1 and Zfp281 act together in promoting the naive to primed transition and safeguarding primed pluripotency by inhibiting the naive cell fate (Figure 7G). Like Tet1 (Wu et al., 2011), Zfp281 exerts dual functions in transcriptional regulation of primed pluripotency, which is exemplified by activation of the primed specific gene *miR-302/367* and repression of the naive specific gene *Tet2* (Figure 5J and Figure 7G).

Although global analyses of DNA methylation and relative Tet1 and Tet2 expression in 2iL and SL ESCs revealed dynamic changes of both 5hmC and Tet1/2 transcriptional levels during the time course of 2iL and SL conversion (Ficz et al., 2013; Habibi et al., 2013; Hackett et al., 2013; Leitch et al., 2013), our study for the first time elucidates how Tet1 can play a critical role in primed pluripotency and how Tet2 is regulated (i.e., repressed) at both the transcriptional and post-transcriptional levels in primed cells to safeguard primed pluripotency. It was proposed that demethylation involves oxidation, replicative loss, and repression of de novo methyltransferases Dnmt3a/b by Nanog and/or Prdm14 in 2iL naive ESCs (Ficz et al., 2013; Habibi et al., 2013; Hackett et al., 2013; Leitch et al., 2013). Our study advocates regulatory roles of the key pluripotency factor Zfp281 in suppressing naive pluripotency and promoting primed pluripotency by activation of a subset of primed genes via recruitment of Tet1 and its DNA demethylation activity and repression of naive genes, exemplified by *Tet2*, through a dual HDAC2 and miR-302/367 repression mechanism (Figure 5J and Figure 7G). Such a model was further supported by a close physical association of Zfp281 with the epigenetic regulators HDAC2, Tet1, and Sin3a in EpiSCs (Figure S7J). Future studies using ChIP-seq to interrogate global binding profiles of both Tet1 and Zfp281 under FA conditions or in EpiSCs will be instrumental to further define how Zfp281 coordinates Tet1 functions in chromatin and target gene regulation, globally or locally, during the establishment and maintenance of primed pluripotency. Because Zfp281, in addition to Otx2, was also reported to be associated with primed specific function of Oct4 in EpiLCs (Buecker et al., 2014), whether it can function together with or independently of Otx2 in affecting Oct4 binding and reshaping core pluripotency factor binding profiles during naive to primed state transition is worthy of future investigation. In this regard, an Otx2-independent function of Zfp281 is most likely due to the lack of a physical association between Zfp281 and Otx2 (Figure 6B).

Distinct roles of Tet1 and Tet2 in pluripotency and reprogramming have been suggested in the literature, although a detailed molecular understanding is lacking. While mapping 5hmC global

---

complexes to shared loci, leading to transcriptional activation of primed and repression of naive genes. In contrast, the downregulation of Zfp281 during naive pluripotent transition releases the *Tet2* transcriptional and post-transcriptional (via primed specific *miR-302/367*) repression (Figure 5J), leading to Tet2 upregulation and naive gene activation.
See also Figure S7.

distribution in Tet1- versus Tet2-depleted mouse ESCs, Huang et al. reported distinct roles for Tet1 and Tet2 in regulating promoter, exon, and polyadenylation site usage (Huang et al., 2014). While performing fusion reprogramming, Piccolo et al. found that Tet1 was critically required for imprint erasure during embryonic germ cell (EGC) and somatic cell fusion, whereas Tet2 was only required for the efficient reprogramming capacity of EGCs by upregulating pluripotency-associated genes after fusion (Piccolo et al., 2013). In contrast, imprinting is stably maintained in mouse ESC and somatic cell fusion, and a rapid accumulation of 5hmC was observed at pluripotency loci (e.g., Oct4) with a primary involvement of Tet2 function as observed in EGC and somatic cell fusion (Piccolo et al., 2013). These fusion reprogramming data lend further support on our findings that Tet2 promotes naive pluripotency, although it remains to be seen whether and how distinct functions of Tet1/2 may play a role in imprinting control during pluripotent state transition. In this regard, it is noteworthy that potential issues were recently reported (Gkountela et al., 2015; Pastor et al., 2016) to associate with the two well-recognized naive hESCs reverted from their conventional primed counterparts (Takashima et al., 2014; Theunissen et al., 2014), including the hotspots of "unbridled DNA demethylation," a non-blastocyst DNA methylation pattern, and a near-total loss of imprinting. Therefore, understanding the molecular determinants of primed and naive pluripotency encompassing ZNF281 and TET1/2 proteins and their mechanistic action in hESCs warrants further investigation.

EXPERIMENTAL PROCEDURES

Additional experimental procedures are provided in Supplemental Experimental Procedures.

Blastocyst Injection

See Supplemental Experimental Procedures for detail. All mouse procedures were performed in accordance with Mount Sinai IACUC policy. Blastocyst injection and chimera formation were performed in the Mouse Genetic Shared Research Facility (SRF) at Mount Sinai.

In Vitro Metastable to Naive and Primed Pluripotent Cell Fate Conversions

For conversion of mouse metastable pluripotent ESCs (SL) into naive or primed pluripotent cells, 3×10^4 cells/cm^2 were seeded on 0.1% gelatin-coated plates using 2iL culture conditions or fibronectin-coated plates using FA culture conditions. Converted cells were passaged with Accutase (Innovative Cell Technologies) at a 1:6 ratio every 2 days. Details of cell culture are given in Supplemental Experimental Procedures.

Ectopic Expression and Endogenous Repression of miR-302/367

The miR-302/367 cluster was overexpressed by retroviral infection of pMIGR1-miR-302/367 construct, and endogenous miR-302/367 was repressed by lentiviral infection with the vector pLenti-EF12-KRAB-302 s-TALE1. Infected cells were sorted using fluorescence-activated cell sorting (FACS) according to the expression of GFP, and RNA was extracted and processed for expression analysis using qPCR.

Luciferase Assay

Zfp281 KO and WT ESCs were transfected with psiCheck2 empty vector or containing Tet2 3′ UTR, as previously reported (Cheng et al., 2013). 24 hr after transfection, the cells were cultured in 2iL, SL, or FA medium for another 24 hr. Luciferase and Renilla activity were determined using Dual-Glo Luciferase Assay kit (#E2920, Promega) according to manufacturer's instructions.

ChIP Coupled with Sequencing

ChIP was performed as previously described (Lee et al., 2006) by using Zfp281 antibody (ab101318, Abcam) in SL ESCs. Detailed analysis can be found in Supplemental Experimental Procedures. High-throughput sequencing HiSeq2500 (Illumina) was performed in Mount Sinai Sequencing Core Facility.

RNA-Seq and Analysis

Two biological replicates of RNA-seq for Zfp281 KO and WT ESCs cultured 48 hr in SL, 2iL, or FA conditions, and WT ESCs under long culture in 2iL (16 days) and stable EpiSCs in FA medium, respectively, were performed. See detailed analysis in Supplemental Experimental Procedures.

ACCESSION NUMBERS

The accession number for the Zfp281 ChIP-seq and RNA-seq data in mouse ESCs reported in this paper is GEO: GSE81045.

SUPPLEMENTAL INFORMATION

Supplemental Information includes Supplemental Experimental Procedures, seven figures, and six tables and can be found with this article online at http://dx.doi.org/10.1016/j.stem.2016.05.025.

AUTHOR CONTRIBUTIONS

M.F. conceived, designed, and conducted the studies and wrote the manuscript; D.G., C.S.-P., V.J.V., A.S., J.D., W.-S.W., and C.C. provided reagents and performed experiments; X.H. provided bioinformatics support; and J.W. conceived the project, designed the experiments, and prepared and approved the manuscript.

ACKNOWLEDGMENTS

REFERENCES

Bao, S., Tang, F., Li, X., Hayashi, K., Gillich, A., Lao, K., and Surani, M.A. (2009). Epigenetic reversion of post-implantation epiblast to pluripotent embryonic stem cells. Nature 461, 1292–1295.

Betschinger, J., Nichols, J., Dietmann, S., Corrin, P.D., Paddison, P.J., and Smith, A. (2013). Exit from pluripotency is gated by intracellular redistribution of the bHLH transcription factor Tfe3. Cell 153, 335–347.

Brons, I.G., Smithers, L.E., Trotter, M.W., Rugg-Gunn, P., Sun, B., Chuva de Sousa Lopes, S.M., Howlett, S.K., Clarkson, A., Ahrlund-Richter, L., Pedersen, R.A., and Vallier, L. (2007). Derivation of pluripotent epiblast stem cells from mammalian embryos. Nature 448, 191–195.

Buecker, C., Srinivasan, R., Wu, Z., Calo, E., Acampora, D., Faial, T., Simeone, A., Tan, M., Swigut, T., and Wysocka, J. (2014). Reorganization of enhancer patterns in transition from naive to primed pluripotency. Cell Stem Cell 14, 838–853.

Chan, Y.S., Göke, J., Ng, J.H., Lu, X., Gonzales, K.A., Tan, C.P., Tng, W.Q., Hong, Z.Z., Lim, Y.S., and Ng, H.H. (2013). Induction of a human pluripotent state with distinct regulatory circuitry that resembles preimplantation epiblast. Cell Stem Cell 13, 663–675.

Chen, Q., Chen, Y., Bian, C., Fujiki, R., and Yu, X. (2013). TET2 promotes histone O-GlcNAcylation during gene transcription. Nature 493, 561–564.

Chen, Y., Niu, Y., Li, Y., Ai, Z., Kang, Y., Shi, H., Xiang, Z., Yang, Z., Tan, T., Si, W., et al. (2015). Generation of Cynomolgus Monkey Chimeric Fetuses using Embryonic Stem Cells. Cell Stem Cell 17, 116–124.

Cheng, J., Guo, S., Chen, S., Mastriano, S.J., Liu, C., D'Alessio, A.C., Hysolli, E., Guo, Y., Yao, H., Megyola, C.M., et al. (2013). An extensive network of TET2-targeting microRNAs regulates malignant hematopoiesis. Cell Rep. 5, 471–481.

Chou, Y.F., Chen, H.H., Eijpe, M., Yabuuchi, A., Chenoweth, J.G., Tesar, P., Lu, J., McKay, R.D., and Geijsen, N. (2008). The growth factor environment defines distinct pluripotent ground states in novel blastocyst-derived stem cells. Cell 135, 449–461.

Clark, A.T. (2015). DNA methylation remodeling in vitro and in vivo. Curr. Opin. Genet. Dev. 34, 82–87.

Costa, Y., Ding, J., Theunissen, T.W., Faiola, F., Hore, T.A., Shliaha, P.V., Fidalgo, M., Saunders, A., Lawrence, M., Dietmann, S., et al. (2013). NANOG-dependent function of TET1 and TET2 in establishment of pluripotency. Nature 495, 370–374.

Dawlaty, M.M., Breiling, A., Le, T., Barrasa, M.I., Raddatz, G., Gao, Q., Powell, B.E., Cheng, A.W., Faull, K.F., Lyko, F., and Jaenisch, R. (2014). Loss of Tet enzymes compromises proper differentiation of embryonic stem cells. Dev. Cell 29, 102–111.

Ding, J., Xu, H., Faiola, F., Ma'ayan, A., and Wang, J. (2012). Oct4 links multiple epigenetic pathways to the pluripotency network. Cell Res. 22, 155–167.

Ding, J., Huang, X., Shao, N., Zhou, H., Lee, D.F., Faiola, F., Fidalgo, M., Guallar, D., Saunders, A., Shliaha, P.V., et al. (2015). Tex10 Coordinates Epigenetic Control of Super-Enhancer Activity in Pluripotency and Reprogramming. Cell Stem Cell 16, 653–668.

Factor, D.C., Corradin, O., Zentner, G.E., Saiakhova, A., Song, L., Chenoweth, J.G., McKay, R.D., Crawford, G.E., Scacheri, P.C., and Tesar, P.J. (2014). Epigenomic comparison reveals activation of "seed" enhancers during transition from naive to primed pluripotency. Cell Stem Cell 14, 854–863.

Ficz, G., Hore, T.A., Santos, F., Lee, H.J., Dean, W., Arand, J., Krueger, F., Oxley, D., Paul, Y.L., Walter, J., et al. (2013). FGF signaling inhibition in ESCs drives rapid genome-wide demethylation to the epigenetic ground state of pluripotency. Cell Stem Cell 13, 351–359.

Fidalgo, M., Shekar, P.C., Ang, Y.S., Fujiwara, Y., Orkin, S.H., and Wang, J. (2011). Zfp281 functions as a transcriptional repressor for pluripotency of mouse embryonic stem cells. Stem Cells 29, 1705–1716.

Gafni, O., Weinberger, L., Mansour, A.A., Manor, Y.S., Chomsky, E., Ben-Yosef, D., Kalma, Y., Viukov, S., Maza, I., Zviran, A., et al. (2013). Derivation of novel human ground state naive pluripotent stem cells. Nature 504, 282–286.

Galonska, C., Ziller, M.J., Karnik, R., and Meissner, A. (2015). Ground state conditions induce rapid reorganization of core pluripotency factor binding before global epigenetic reprogramming. Cell Stem Cell 17, 462–470.

Gkountela, S., Zhang, K.X., Shafiq, T.A., Liao, W.W., Hargan-Calvopiña, J., Chen, P.Y., and Clark, A.T. (2015). DNA demethylation dynamics in the human prenatal germline. Cell 161, 1425–1436.

Guo, G., Yang, J., Nichols, J., Hall, J.S., Eyres, I., Mansfield, W., and Smith, A. (2009). Klf4 reverts developmentally programmed restriction of ground state pluripotency. Development 136, 1063–1069.

Habibi, E., Brinkman, A.B., Arand, J., Kroeze, L.I., Kerstens, H.H., Matarese, F., Lepikhov, K., Gut, M., Brun-Heath, I., Hubner, N.C., et al. (2013). Whole-genome bisulfite sequencing of two distinct interconvertible DNA methylomes of mouse embryonic stem cells. Cell Stem Cell 13, 360–369.

Hackett, J.A., and Surani, M.A. (2014). Regulatory principles of pluripotency: from the ground state up. Cell Stem Cell 15, 416–430.

Hackett, J.A., Dietmann, S., Murakami, K., Down, T.A., Leitch, H.G., and Surani, M.A. (2013). Synergistic mechanisms of DNA demethylation during transition to ground-state pluripotency. Stem Cell Reports 1, 518–531.

Han, D.W., Tapia, N., Joo, J.Y., Greber, B., Araúzo-Bravo, M.J., Bernemann, C., Ko, K., Wu, G., Stehling, M., Do, J.T., and Schöler, H.R. (2010). Epiblast stem cell subpopulations represent mouse embryos of distinct pregastrulation stages. Cell 143, 617–627.

Hockemeyer, D., Wang, H., Kiani, S., Lai, C.S., Gao, Q., Cassady, J.P., Cost, G.J., Zhang, L., Santiago, Y., Miller, J.C., et al. (2011). Genetic engineering of human pluripotent cells using TALE nucleases. Nat. Biotechnol. 29, 731–734.

Huang, X., and Wang, J. (2014). The extended pluripotency protein interactome and its links to reprogramming. Curr. Opin. Genet. Dev. 28, 16–24.

Huang, Y., Chavez, L., Chang, X., Wang, X., Pastor, W.A., Kang, J., Zepeda-Martínez, J.A., Pape, U.J., Jacobsen, S.E., Peters, B., and Rao, A. (2014). Distinct roles of the methylcytosine oxidases Tet1 and Tet2 in mouse embryonic stem cells. Proc. Natl. Acad. Sci. USA 111, 1361–1366.

Lee, T.I., Johnstone, S.E., and Young, R.A. (2006). Chromatin immunoprecipitation and microarray-based analysis of protein location. Nat. Protoc. 1, 729–748.

Leitch, H.G., McEwen, K.R., Turp, A., Encheva, V., Carroll, T., Grabole, N., Mansfield, W., Nashun, B., Knezovich, J.G., Smith, A., et al. (2013). Naive pluripotency is associated with global DNA hypomethylation. Nat. Struct. Mol. Biol. 20, 311–316.

MacArthur, B.D., Sevilla, A., Lenz, M., Müller, F.J., Schuldt, B.M., Schuppert, A.A., Ridden, S.J., Stumpf, P.S., Fidalgo, M., Ma'ayan, A., et al. (2012). Nanog-dependent feedback loops regulate murine embryonic stem cell heterogeneity. Nat. Cell Biol. 14, 1139–1147.

Marks, H., Kalkan, T., Menafra, R., Denissov, S., Jones, K., Hofemeister, H., Nichols, J., Kranz, A., Stewart, A.F., Smith, A., and Stunnenberg, H.G. (2012). The transcriptional and epigenomic foundations of ground state pluripotency. Cell 149, 590–604.

Nichols, J., and Smith, A. (2009). Naive and primed pluripotent states. Cell Stem Cell 4, 487–492.

Orkin, S.H. (2005). Chipping away at the embryonic stem cell network. Cell 122, 828–830.

Pastor, W.A., Chen, D., Liu, W., Kim, R., Sahakyan, A., Lukianchikov, A., Plath, K., Jacobsen, S.E., and Clark, A.T. (2016). Naive human pluripotent cells feature a methylation landscape devoid of blastocyst or germline memory. Cell Stem Cell 18, 323–329.

Piccolo, F.M., Bagci, H., Brown, K.E., Landeira, D., Soza-Ried, J., Feytout, A., Mooijman, D., Hajkova, P., Leitch, H.G., Tada, T., et al. (2013). Different roles for Tet1 and Tet2 proteins in reprogramming-mediated erasure of imprints induced by EGC fusion. Mol. Cell 9, 1023–1033.

Takashima, Y., Guo, G., Loos, R., Nichols, J., Ficz, G., Krueger, F., Oxley, D., Santos, F., Clarke, J., Mansfield, W., et al. (2014). Resetting transcription factor control circuitry toward ground-state pluripotency in human. Cell 158, 1254–1269.

Theunissen, T.W., Powell, B.E., Wang, H., Mitalipova, M., Faddah, D.A., Reddy, J., Fan, Z.P., Maetzel, D., Ganz, K., Shi, L., et al. (2014). Systematic identification of culture conditions for induction and maintenance of naive human pluripotency. Cell Stem Cell 15, 471–487.

Wang, J., Rao, S., Chu, J., Shen, X., Levasseur, D.N., Theunissen, T.W., and Orkin, S.H. (2006). A protein interaction network for pluripotency of embryonic stem cells. Nature 444, 364–368.

Weinberger, L., Ayyash, M., Novershtern, N., and Hanna, J.H. (2016). Dynamic stem cell states: naive to primed pluripotency in rodents and humans. Nat. Rev. Mol. Cell Biol. 17, 155–169.

Wu, J., and Izpisua Belmonte, J.C. (2015). Dynamic pluripotent stem cell states and their applications. Cell Stem Cell 17, 509–525.

Wu, H., D'Alessio, A.C., Ito, S., Xia, K., Wang, Z., Cui, K., Zhao, K., Sun, Y.E., and Zhang, Y. (2011). Dual functions of Tet1 in transcriptional regulation in mouse embryonic stem cells. Nature 473, 389–393.

Wu, J., Okamura, D., Li, M., Suzuki, K., Luo, C., Ma, L., He, Y., Li, Z., Benner, C., Tamura, I., et al. (2015). An alternative pluripotent state confers interspecies chimaeric competency. Nature 521, 316–321.